Efficient Vision-Based Calibration for Visual Surveillance Systems with Multiple PTZ Cameras

I-Hsien Chen and Sheng-Jyh Wang

Department of Electronics Engineering, Institute of Electronics, National Chiao Tung University,
Hsinchu, Taiwan, R.O.C.
kace.ee89g@nctu.edu.tw, shengjyh@cc.nctu.edu.tw

Abstract

Surveillance systems with multiple cameras have become increasingly important. The space relationship between cameras offers useful information for surveillance applications, such as object tracking or 3-D positioning. In this paper, we propose a vision-based approach to infer the relative positioning and orientation among multiple PTZ cameras. The relationship between the tilt angle of a PTZ camera and the 3D-to-2D coordinate transformation is built first. Then, the tilt angles and the altitudes of PTZ cameras are estimated based on the observation of some simple objects lying on a horizontal plane, with known intrinsic parameters of these PTZ cameras. With the estimated tilt angles and altitudes, the calibration of multiple cameras can be accomplished by comparing the back-projected world coordinates of a common vector in the 3-D space. The whole procedure does not need a huge amount of data and the computational load is light. Experimental results over real images have demonstrated the efficiency and feasibility of this approach.

1. Introduction

PTZ (Pan-tilt-zoom) cameras are commonly used in surveillance systems. Even though the use of PTZ cameras provides the capability to conveniently change the view of monitoring or to dynamically follow monitored objects, the calibration of the extrinsic parameters for these PTZ cameras is inherently a difficult problem. Even though various kinds of approaches have already been developed to calibrate the intrinsic and extrinsic parameters of static cameras [1-9], it would be impractical to repeatedly perform these elaborate calibration processes over a PTZ camera when that camera is under panning, tilting, or zooming all the time.

The situation becomes even more complicated when more than two PTZ cameras are used in a visual surveillance system. For this case, due to the time-varying relationships among PTZ cameras, a practical calibration method should not only be efficient but also need no particular system setup. Hence, even though some calibration methods have already been proposed to calibrate multiple static cameras [10-12], those methods are still too complicated to be practically used for the calibration of multiple PTZ cameras. In this paper, we'll propose a novel and efficient method to accomplish the calibration of multiple PTZ cameras. This method doesn't require particular pattern grid or specific camera setup. Moreover, it does not need a large amount of data and the computational load is pretty low.

For a PTZ camera, the position, orientation, and shape of projected objects on the image plane may change accordingly whenever there is a change in pan angle or tilt angle. In our approach, we first deduce the 3D-to-2D coordinate transformation in terms of the tilt angle of a PTZ camera. Based on the 3D-to-2D transformation, we'll propose an efficient method to infer the tilt angle and altitude of each PTZ camera based on the observation of some simple objects lying on a horizontal plane. The estimated tilt angle and altitude offer a direct geometric sense about the pose of PTZ camera. Then, based on some 3-D vectors commonly observed by these PTZ cameras, the calibration of multiple PTZ cameras can be easily achieved.

This paper is organized as follows. First, in Section 2, the camera model of our surveillance system is described. In Section 3, we'll develop the mapping between the 3-D space and the 2-D image plane in terms of tilt angle, under the constraint that all observed points are lying on a horizontal plane. Based on the back projection formula, the tilt angle and altitude of a camera can thus be estimated by viewing

some simple patterns on a horizontal plane. Then, in Section 4, we'll introduce the calibration of multiple cameras. Finally, in Section 5, some experimental results over real data are demonstrated to illustrate the feasibility of this method.

2. Camera model

In this section, we'll give a sketch of our camera model, including the system overview, the model of camera setup, and the basic camera projection model. Although the camera model is built according to our surveillance environment, it is general enough to fit for a large class of surveillance scenes equipped with multiple PTZ cameras.

2.1. System overview

In the setup of our indoor surveillance system, four PTZ cameras are mounted on the ceiling of our lab, about 3 meters above the ground plane. The lab is full of desks, chairs, PC computers, and monitors. All the tabletops are roughly parallel to the ground plane. In this paper, we'll propose a simple method to estimate the tilt angles and altitudes of PTZ cameras based on the images of a few corners with fixed angles, or a few line segments with fixed length. These corners and line segments are to be placed on a horizontal plane, like a desktop. Fig. 8 shows a simple example, where we observe the corners and boundaries of a few A4 paper sheets on a tabletop. Based on this simple setup, we'll demonstrate that the tilt angles and the heights of these four PTZ cameras can be easily estimated. Then, after the estimations of tilt angles and heights, the calibration of these four PTZ cameras can be easily achieved. In Fig. 1, we show the flowchart of the proposed calibration procedure.

2.2. Scene model

Fig. 2 illustrates the modeling of our camera setup. Here, we assume the observed objects locate on a horizontal plane $\prod$, while the PTZ camera lies with a height h above $\prod$. The PTZ camera may pan or tilt with respect to the rotation center O_R. Moreover, we assume the projection center of the camera, denoted as O_C, is away from O_R with distance r. To simplify the deduction of the following formulae, we define the origin of the rectified world coordinates to be the projection center O_C of a PTZ camera with zero tilt angle. The Z-axis of the world coordinates is along the optical axis of the camera, while the X- and Y-axis of the world coordinates are parallel to the x- and y-axis

of the projected image plane, respectively, as shown in Fig. 2. When the camera tilts, the projection center moves to O_C' and the projected image plane is changed to a new 2-D plane. In this case, the y-axis of the image plane is no longer parallel to the Y-axis of the world coordinates, while the x-axis is still parallel to the X-axis.
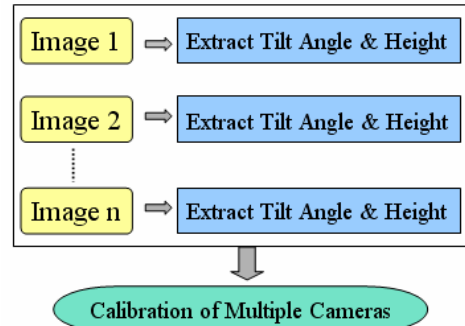
Figure 1. Flowchart
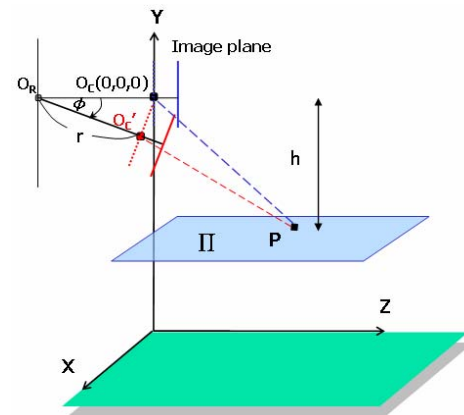
Figure 2. Scene model

2.3. Basic equations

Assume $P=[X, Y, Z, 1]^T$ denotes the homogeneous coordinates of a 3-D point **p** in the world coordinates. For the case of a PTZ camera with zero tilt angle, we denote the perspective projection of **p** as $p= [x, y, 1]^T$. Under perspective projection, we have

$$p = \frac{1}{Z}\begin{bmatrix} \alpha & s & u_0 \\ 0 & \beta & v_0 \\ 0 & 0 & 1 \end{bmatrix}\begin{bmatrix} R & t \end{bmatrix}P \quad , \tag{1}$$

where α and β are the scale parameters expressed in pixel units for the x and y axes in the image plane, s is the skew factor due to some manufacturing error, and (u_0, v_0) is the principal point [13].

With respect to the rectified world coordinate system, the extrinsic term $[R \ t]$ becomes $[I \ 0]$. To

further simplify the mathematical deduction, we ignore the skew factor s and assume the image coordinates have been translated by a translation vector ($-u_0$, $-v_0$). Hence, Eq. (1) can be simplified as

$$\begin{bmatrix} x \\ y \\ 1 \end{bmatrix} = \frac{1}{Z}\begin{bmatrix} \alpha & 0 & 0 \\ 0 & \beta & 0 \\ 0 & 0 & 1 \end{bmatrix}\begin{bmatrix} X \\ Y \\ Z \end{bmatrix}, \tag{2}$$

or in a reverse way as

$$\begin{bmatrix} X \\ Y \\ Z \end{bmatrix} = Z\begin{bmatrix} 1/\alpha & 0 & 0 \\ 0 & 1/\beta & 0 \\ 0 & 0 & 1 \end{bmatrix}\begin{bmatrix} x \\ y \\ 1 \end{bmatrix} = \begin{bmatrix} xZ/\alpha \\ yZ/\beta \\ Z \end{bmatrix}. \tag{3}$$

3. Estimating the pose of PTZ cameras

3.1. Coordinate mapping on a tilted camera

When a PTZ camera tilts with an angle ϕ, the projection center O_C translates to a new place O_C' with $O_C' = [0\ -r\sin\phi\ -(r-r\cos\phi)]^T$. Assume we define a tilted world coordinate system (X', Y', Z') with respect to the tilted camera, with the origin being the new project center O_C', the Z'-axis being the optical axis of the tilted camera, and the X'- and Y'-axis being parallel to the x'- and y'-axis of the new projected image plane, respectively. Then, it can be easily deduced that in the tilted world coordinate system the coordinates of the 3-D point **p** become

$$\begin{bmatrix} X' \\ Y' \\ Z' \end{bmatrix} = \begin{bmatrix} 1 & 0 & 0 \\ 0 & \cos\phi & \sin\phi \\ 0 & -\sin\phi & \cos\phi \end{bmatrix}\begin{bmatrix} X \\ Y+r\sin\phi \\ Z+r(1-\cos\phi) \end{bmatrix}$$
$$= \begin{bmatrix} X \\ Y\cos\phi+Z\sin\phi+r\sin\phi \\ -Y\sin\phi+Z\cos\phi+r(\cos\phi-1) \end{bmatrix}. \tag{4}$$

Then, after applying the perspective projection formula, the homogeneous coordinates of the projected image point now move to

$$\begin{bmatrix} x' \\ y' \\ 1 \end{bmatrix} = \begin{bmatrix} \alpha\dfrac{X'}{Z'} \\ \beta\dfrac{Y'}{Z'} \\ 1 \end{bmatrix} = \begin{bmatrix} \alpha\dfrac{X}{-Y\sin\phi+Z\cos\phi+r(\cos\phi-1)} \\ \beta\dfrac{Y\cos\phi+Z\sin\phi+r\sin\phi}{-Y\sin\phi+Z\cos\phi+r(\cos\phi-1)} \\ 1 \end{bmatrix}. \tag{5}$$

3.2. Constrained coordinate mapping

In the rectified world coordinates, all points on a horizontal plane have the same Y coordinate. That is, $Y = -h$ for a constant h. The homogeneous form of this plane $\prod$ can be defined as $\pi = [0\ 1\ 0\ h]^T$. Assume the PTZ camera is tilted with an angle ϕ. Then, in the tilted world coordinate system, the homogeneous form of this plane $\prod$ becomes $\pi' = [0\ \cos\phi\ -\sin\phi\ (h-r\sin\phi)]^T$.
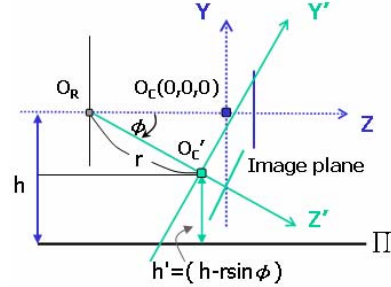
Figure 3. Geometry of a horizontal plane with respect to a rectified camera and a tilted camera

Assume a 3-D point **p** locates on the horizontal plane $\prod$. Then, in the rectified world coordinate system, we have $\pi \bullet P = 0$, where $P = [X, Y, Z, 1]^T$. Similarly, in the tilted world coordinate system, we have $\pi' \bullet P' = 0$, where $P' = [X', Y', Z', 1]^T$. With Eq. (3), the constraint function becomes

$$\begin{bmatrix} 0 & \cos\phi & -\sin\phi & (h-r\sin\phi) \end{bmatrix}\begin{bmatrix} x'Z'/\alpha \\ y'Z'/\beta \\ Z' \\ 1 \end{bmatrix} = 0. \tag{6}$$

By solving (6), Z' is found to be

$$Z' = \frac{\beta(r\sin\phi-h)}{y'\cos\phi-\beta\sin\phi}. \tag{7}$$

Moreover, the tilted world coordinates of **p** become

$$\begin{bmatrix} X' \\ Y' \\ Z' \end{bmatrix} = \begin{bmatrix} \dfrac{x'\beta(r\sin\phi-h)}{\alpha(y'\cos\phi-\beta\sin\phi)} \\ \dfrac{y'(r\sin\phi-h)}{y'\cos\phi-\beta\sin\phi} \\ \dfrac{\beta(r\sin\phi-h)}{y'\cos\phi-\beta\sin\phi} \end{bmatrix}. \tag{8}$$

With Equations (4) and (8), we may transfer $[X', Y', Z']^T$ back to $[X, Y, Z]^T$ to obtain

$$\begin{bmatrix} X \\ Y \\ Z \end{bmatrix} = \begin{bmatrix} \dfrac{x'\beta(r\sin\phi-h)}{\alpha(y'\cos\phi-\beta\sin\phi)} \\ -h \\ \dfrac{(y'\sin\phi+\beta\cos\phi)(r\sin\phi-h)}{y'\cos\phi-\beta\sin\phi}-r+r\cos\phi \end{bmatrix}. \tag{9}$$

If the principal point is taken into account, then (9) can be reformulated as

$$\begin{bmatrix} X \\ Y \\ Z \end{bmatrix} = \begin{bmatrix} \dfrac{(x'-u_0)\beta(r\sin\phi - h)}{\alpha[(v_0 - y')\cos\phi - \beta\sin\phi]} \\ -h \\ \dfrac{[(v_0 - y')\sin\phi + \beta\cos\phi](r\sin\phi - h)}{(v_0 - y')\cos\phi - \beta\sin\phi} - r + r\cos\phi \end{bmatrix}.\textbf{(10)}$$

This formula indicates the back projection formula from the image coordinates of a tilted camera to the rectified world coordinates, under the constraint that all the observed points are lying on a horizontal plane with $Y = -h$.

3.3. Estimation of tilt angle based on back-projections

In real life, based on the image contents of a captured image, people could usually have a rough estimate about the relative position of the camera with respect to the captured objects. In this section, we propose a simple method based on this observation. Here, we'll demonstrate how we can easily estimate the tilt angle of the camera based on the back projection of the captured images of a few corners or line segments.

(a)

(b)
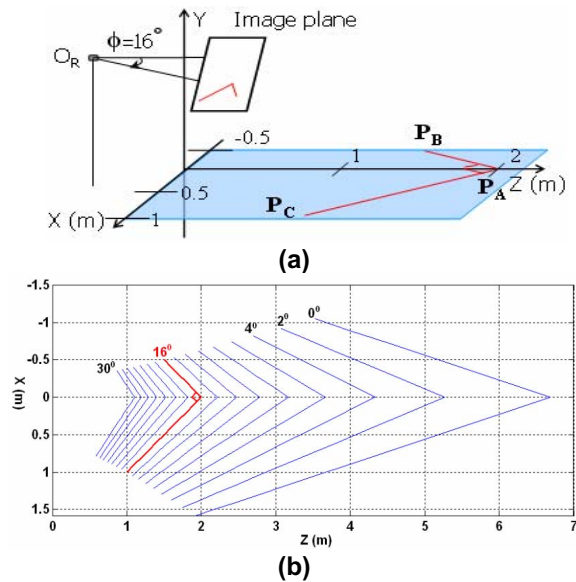
Figure 4. (a) Rectangular corner captured by a tilted camera (b) Illustration of back-projection onto a horizontal plane on for different choices of tilt angles.

Imagine we use a tilted camera to capture the image of a corner, which is locating on a horizontal plane. Based on the captured image and a guessed tilt angle,

(a)

(b)
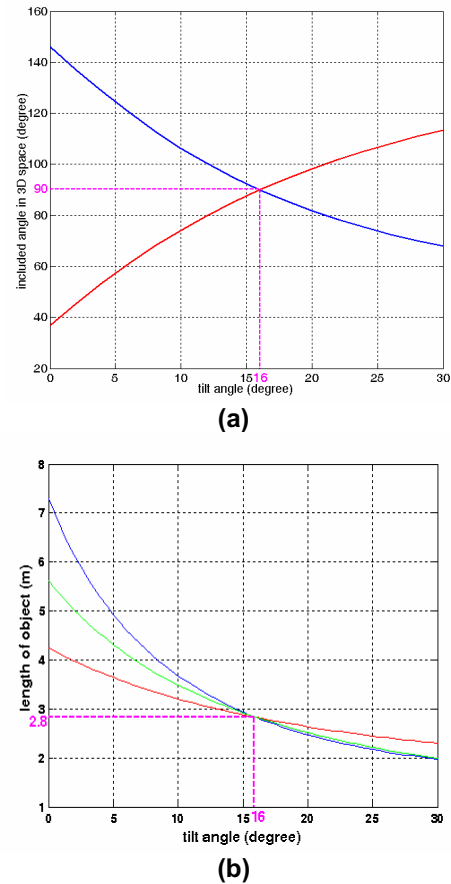
Figure 5. (a)Back-projected angle and (b) Back-projected length with respect to different choices of tilt angles

we may use (10) to back-project the captured image onto a horizontal plane on $Y = -h$. Assume three 3-D points, P_A, P_B, and P_C, on a horizontal plane form a rectangular corner at P_A. The original image is captured by a camera with $\phi = 16^\circ$, as shown in Fig. 4(a). In Fig. 4(b), we plot the back-projected images for various choices of tilt angles. The guessed tilt angles range from 0 to 30 degrees, with a 2-degree step. The back-projection for the choice of 16° is plotted in red, specifically. It can be seen that the back-projected corner becomes a rectangular corner only if the guessed tilt angle is correct. Besides, it is worth mentioning that a different choice of h only causes a scaling effect of the back-projected shape.

To formulate this example, we assume the corner at P_A with an angle ψ. Besides, P_A and P_B form a line segment with length L. The angle ψ and length L can be calculated based on the following formula:

$$\cos\psi = \frac{\left\langle \overline{P_A P_B}, \overline{P_A P_C} \right\rangle}{\left\| \overline{P_A P_B} \right\| \times \left\| \overline{P_A P_C} \right\|} \text{ and } \left\| \overline{P_A P_B} \right\| = L. \qquad (11)$$

After capturing the image of these three points, we can use their image coordinates and Eq. (10) to build the relation between the back-projected angle and the guessed tilt angle:

$$\psi = \cos^{-1}\left\{\left\{\left(\frac{x_B'\beta}{\alpha(y_B'\cos\phi - \beta\sin\phi)} - \frac{x_A'\beta}{\alpha(y_A'\cos\phi - \beta\sin\phi)}\right)\right.\right.$$
$$\times\left(\frac{x_C'\beta}{\alpha(y_C'\cos\phi - \beta\sin\phi)} - \frac{x_A'\beta}{\alpha(y_A'\cos\phi - \beta\sin\phi)}\right)$$
$$+\left(\frac{(y_B'\sin\phi + \beta\cos\phi)}{y_B'\cos\phi - \beta\sin\phi} - \frac{(y_A'\sin\phi + \beta\cos\phi)}{y_A'\cos\phi - \beta\sin\phi}\right)$$
$$\times\left.\left(\frac{(y_C'\sin\phi + \beta\cos\phi)}{y_C'\cos\phi - \beta\sin\phi} - \frac{(y_A'\sin\phi + \beta\cos\phi)}{y_A'\cos\phi - \beta\sin\phi}\right)\right\}$$
$$\times\left\{\left(\frac{x_B'\beta}{\alpha(y_B'\cos\phi - \beta\sin\phi)} - \frac{x_A'\beta}{\alpha(y_A'\cos\phi - \beta\sin\phi)}\right)^2\right.$$
$$+\left.\left(\frac{y_B'\sin\phi + \beta\cos\phi}{y_B'\cos\phi - \beta\sin\phi} - \frac{y_A'\sin\phi + \beta\cos\phi}{y_A'\cos\phi - \beta\sin\phi}\right)^2\right\}^{-\frac{1}{2}}$$
$$\times\left\{\left(\frac{x_C'\beta}{\alpha(y_C'\cos\phi - \beta\sin\phi)} - \frac{x_A'\beta}{\alpha(y_A'\cos\phi - \beta\sin\phi)}\right)^2\right.$$
$$+\left.\left.\left(\frac{y_C'\sin\phi + \beta\cos\phi}{y_C'\cos\phi - \beta\sin\phi} - \frac{y_A'\sin\phi + \beta\cos\phi}{y_A'\cos\phi - \beta\sin\phi}\right)^2\right\}^{-\frac{1}{2}}\right\}. (12)$$

Note that in (12) we have ignored the offset terms, u_0 and v_0, to reduce the complexity of the formulation. Moreover, the back-projected angle ψ doesn't depend on h and r.

In Fig. 5(a), we show the back-projected angle ψ with respect to the guessed tilt angle, assuming α and β are known in advance. In this simulation, we imagine there is a rectangular corner on a horizontal plane and we capture the image from a tilted camera with $\phi = 16$ degrees. Based on the captured image and different choices of tilt angles, we get different back-projected angles of the corner. The red and blue curves are generated by placing the rectangular corner on two different places of the horizontal plane. Again, the back-projected angle is equal to 90 degrees only if we choose the tilt angle to be 16 degrees. This means if we know in advance the angle of the captured corner, we can easily deduce camera's tilt angle based on (12). Moreover, the red curve and the blue curve intersect at $(\phi, \psi) = (16, 90)$. This means that if we don't know the actual angle of the corner, we can simply place that corner on more than two different places of the horizontal plane. Then, based on the intersection of the deduced ψ -v.s.- ϕ curves, we may not only estimate the tilt angle of the camera but also the actual angle of the corner.

Similarly, we can deduce the relation between the back-projected length and the guessed tilt angle:

$$L = \ell(\phi) = \left\{\left(\frac{(x_B' - u_0)\beta(r\sin\phi - h)}{\alpha[(v_0 - y_B')\cos\phi - \beta\sin\phi]}\right.\right.$$
$$-\left.\frac{(x_A' - u_0)\beta(r\sin\phi - h)}{\alpha[(v_0 - y_A')\cos\phi - \beta\sin\phi]}\right)^2$$
$$+\left(\frac{[(v_0 - y_B')\sin\phi + \beta\cos\phi](r\sin\phi - h)}{(v_0 - y_B')\cos\phi - \beta\sin\phi}\right. \qquad (13)$$
$$-\left.\left.\frac{[(v_0 - y_A')\sin\phi + \beta\cos\phi](r\sin\phi - h)}{(v_0 - y_A')\cos\phi - \beta\sin\phi}\right)^2\right\}^{\frac{1}{2}}$$

Note that in (13), the right-side terms contain a common factor $(r\sin\phi - h)^2$. This means the values of r and h only affect the scaling of L. Hence, we can rewrite the formula as

$$L' \equiv \frac{L}{r\sin\phi - h}$$
$$= \left\{\left(\frac{(x_B' - u_0)\beta}{\alpha[(v_0 - y_B')\cos\phi - \beta\sin\phi]} - \frac{(x_A' - u_0)\beta}{\alpha[(v_0 - y_A')\cos\phi - \beta\sin\phi]}\right)^2 \quad (14)\right.$$
$$+\left.\left(\frac{[(v_0 - y_B')\sin\phi + \beta\cos\phi]}{(v_0 - y_B')\cos\phi - \beta\sin\phi} - \frac{[(v_0 - y_A')\sin\phi + \beta\cos\phi]}{(v_0 - y_A')\cos\phi - \beta\sin\phi}\right)^2\right\}^{\frac{1}{2}}$$

Then, even if the values of r and h are unknown, we may simply place more than two line segments of the same length on different places of a horizontal plane and seek to find the intersection of these corresponding L -v.s.- ϕ curves, as shown in Fig. 5(b).

4. Calibration of multiple cameras

In our camera model, each camera has its own world coordinate system. If a vector in the 3-D space, like a line segment on a tabletop, is observed by several PTZ cameras, we can achieve the calibration of these cameras by mapping the individual back-projected world coordinates of this vector to a common reference world coordinates. In Fig. 6, we take two calibrated PTZ cameras as an example. Fig. 6(a) shows the scene model of these two cameras. Fig. 6(b) shows the vector locations in the world coordinates of these two cameras, respectively. Based on the estimated ϕ and h, and the image projections of the vector points, we can get the world coordinates of points $\mathbf{A_{ref}}$, $\mathbf{B_{ref}}$, and $\mathbf{A'}$, $\mathbf{B'}$ from (10). The difference of the rotation angle ω between the two world coordinate systems can be deduced by

$$\cos\omega = \frac{\left\langle \overline{A'B'}, \overline{A_{ref}B_{ref}} \right\rangle}{\left\| \overline{A'B'} \right\| \times \left\| \overline{A_{ref}B_{ref}} \right\|}.$$

After applying the rotation to point $\mathbf{A'}$, the position translation $\mathbf{t}$ between these two cameras can be expressed as

$$\mathbf{t} = \mathbf{A_{ref}} - \begin{bmatrix} \cos\omega & 0 & -\sin\omega \\ 0 & 1 & 0 \\ \sin\omega & 0 & \cos\omega \end{bmatrix} \cdot \mathbf{A'}. \qquad (15)$$

Hence, the 3-D relationship between these two

cameras can be easily deduced.

(a)

(b)
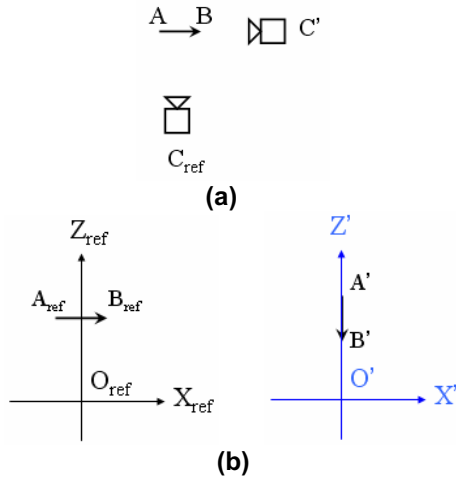
Figure 6. (a) Top view of two calibrated cameras and a vector in the space (b) The world coordinates of the vector in these two cameras

5. Experiments over real images

In the experiments over real images, the test images are to be captured by four PTZ cameras mounted on the ceiling, all with unknown tilt angles and heights. The image resolution is 320 by 240 pixels. Two sheets of A4 paper are randomly placed on a horizontal table, as shown in Fig. 8. The corners of these A4 paper sheets could be easily identified either by hand or by a corner detection algorithm. In the 3-D space, all the corners are 90 degrees, while the length and width of an A4 paper are 297 mm and 210 mm, respectively.

Table 1 lists some experimental results. Note that the distance r between the camera center and the rotation center has no impact over (12) and (14). Even in (13), r tends to have negligible impact since the term $r\sin\phi$ is usually much smaller than h. Hence, the parameter r can be ignored or be estimated via direct measurement. Besides, the intrinsic parameters $\{\alpha, \beta, u_0, v_0\}$ of every camera are estimated in advance, based on Zhang's calibration method [2]. Hence, (13) includes only 2 unknown variables: ϕ and h. Each row corresponds to the mean and standard deviation of the estimated parameters for a different camera. Five observations are made with each observation includes 8 selected line segments on the boundary of these A4 papers, as shown in Fig. 8(a). It can be seen that all the estimated parameters have an acceptable standard deviation. Here, the sensitivities of the estimated ϕ due to parameter and measurement errors are analyzed via simulations. The images are assumed to be captured by

a PTZ camera with tilt angle $\phi = 51$ degrees. When the value of u_0 is changed by an amount of 100, the deduced tilt angle changes about 0.1 degrees. On the other hand, a change of ± 20 pixels in v_0 may cause a 1-degree deviation in the estimated ϕ. Similarly, the estimated ϕ is found to have a ± 1.5- to ± 2-degree fluctuation when the value of β (or α) is changed by the amount of ± 20. Moreover, for measurement errors in image points, a change of $\pm 5\%$ in the measurement of (x', y') may cause a $\pm 6\%$ deviation in the estimated ϕ. Fig. 7 shows such an example of our simulation.

(a)

(b)
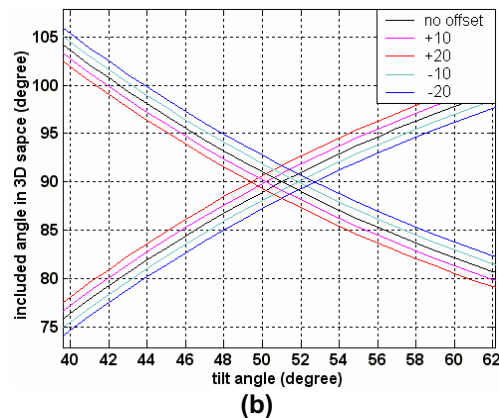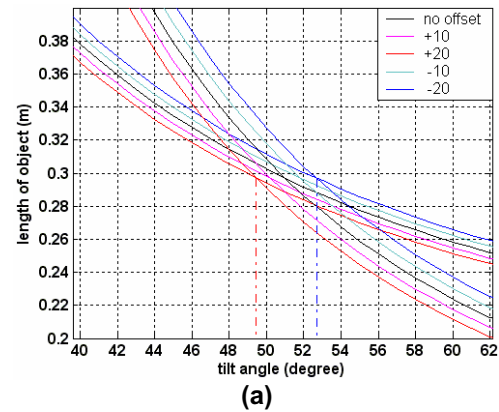
Figure 7. Variations of the (a) L -v.s.-ϕ curves and (b) ψ -v.s.-ϕ curves with respect to the variation of β

In Table 2, each row corresponds to the estimations of the position and orientation of each camera relative to Camera 2. As mentioned in Section 5, the relative position and orientation are computed based on a common vector in Fig. 8(a) and the mean value of ϕ and h. The top view of the relative positions in the 3D space is illustrated in Fig. 9. The coordinate origin is the projection center of Camera 2. Besides, the eight

chosen corners of the A4 papers in Fig. 8(a) are also plotted in Fig. 9 to offer a clearer geometric sense.

To evaluate the calibration results, we randomly pick up a few test points in the image captured by Camera 2 and use the calibration result to find the corresponding points in the other three images. The result is shown in Fig. 8(b), with all corresponding points being represented in the same color. It can be seen that all the corresponding relationships are pretty reasonable. This verifies the credibility and the proposed calibration method.

(a)

(b)

Figure 8. (a) Test image captured by four PTZ cameras (b) Evaluation of the calibration results

6. Conclusion

In summary, in this paper we adopt a system model that is general enough to fit for a large class of surveillance systems with multiple PTZ cameras. It doesn't require particular system setup or specific calibration patterns. If compared with these conventional calibration approaches which extract the

homography and rotation matrices, our approach offers direct geometric sense and can simplify the calibration process for multiple PTZ cameras. In our method, the system setup is simple and the computation load is light. The experiment results over real images do demonstrate the efficiency of this approach.

Table 1. Estimation of tilt angle and height

	Mean		Deviation	
	ϕ(degree)	h(m)	ϕ(degree)	h(m)
Camera 1	20.4	1.96	1.5	0.12
Camera 2	51.1	2.32	0.6	0.03
Camera 3	24.8	1.95	1.2	0.17
Camera 4	44.2	2.01	0.3	0.14

Table 2. Space relationship between cameras

	Relative position & orientation			
	X(m)	Y(m)	Z(m)	ω(degree)
Camera 1	2.7	-0.36	5.70	144.1
Camera 2	0	0	0	0
Camera 3	4.27	-0.37	1.93	87.1
Camera 4	-1.64	-0.31	3.2	-135.4
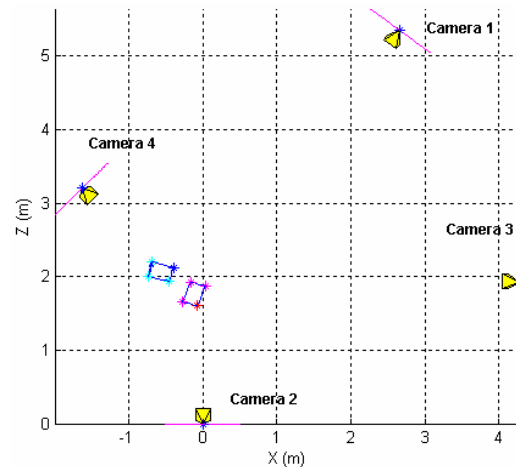
Figure 9. Top view of the relative positions between four PTZ cameras

6. References

[1] Roger Y. Tsai, "A Versatile Camera Calibration Technique for High-Accuracy 3D Machine Vision Metrology Using Off-the-Shelf TV Cameras and Lenses", IEEE Journal of Robotics and Automation, Volume: 3, Issue: 4, Aug 1987, pp. 323-344.

[2] Zhengyou Zhang, "Flexible Camera Calibration by Viewing a Plane from Unknown Orientations", The Proceedings of the Seventh IEEE International Conference on Computer Vision, vol. 1, Sept. 1999, pages 666-673.

[3] Zhengyou Zhang, "Camera Calibration with One-Dimensional Objects", IEEE Transactions on Pattern Analysis and Machine Intelligence, vol. 26, issue 7, July 2004, pp. 892-899.

[4] Motilal Agrawal and Larry S. Davis, "Camera calibration using spheres: A semi-definite programming approach", In Proc. Ninth IEEE International Conference on Computer Vision, vol.2, Oct. 2003, pp. 782-789.

[5] Guo-Qing Wei and Song De Ma, "A Complete Two-Plane Camera Calibration Method and Experimental Comparisons", In Proc. Fourth International Conference on Computer Vision, May 1993, pp. 439-446.

[6] Peter F. Sturm and Stephen J. Maybank, "On Plane-Based Camera Calibration: A General Algorithm, Singularities, Applications", IEEE Computer Society Conference on Computer Vision and Pattern Recognition, Volume 1, June 1999.

[7] Robert T. Collins and Y. Tsin, "Calibration of an Outdoor Active Camera System", IEEE Computer Society Conference on Computer Vision and Pattern Recognition, Volume: 1, June 1999, pp. 534.

[8] A. Basu and K. Ravi, "Active Camera Calibration Using Pan, Tilt and Roll", IEEE Transactions on Systems, Man and Cybernetics, Part B, Volume: 27, Issue: 3, June 1997, pp. 559-566.

[9] Elsayed E. Hemayed, "A Survey of Camera Self-Calibration", In Proc. IEEE Conference on Advanced Video and Signal Based Surveillance, July 2003, pp. 351-357.

[10] Peter Sturm, "Algorithms for Plane-Based Pose Estimation", In Proceedings. IEEE Conference on Computer Vision and Pattern Recognition, Volume 1, June 2000, pp. 706-711.

[11] T. Ueshiba and F. Tomita, "Plane-Based Calibration Algorithm for Multi-Camera Systems via Factorization of Homography Matrices", Proceedings of Ninth IEEE International Conference on Computer Vision, Volume: 2, Oct. 2003, pp. 966-973.

[12] Y. Sugimure and Jun Sato, "Camera Calibration and Reconstruction from the Chain Connection of Mutual Camera Projections", Proceedings of the 17th International Conference on Pattern Recognition, vol. 1, Aug. 2004, pp. 100-103.

[13] D.A. Forsyth and Jean Ponce, Computer Vision: A Modern Approach, Prentice Hall, 2003.